WSe₂ p-MOSFETs with Nb-Doped WS₂ Contacts Deposited using Atomic Layer Deposition

Shivanshu Mishra, Ruixue Li, Dongjea Seo, Anil Adhikari, Lucas G. Cooper, Rebecca A. Dawley, Ageeth A. Bol, and Steven J. Koester, *Fellow, IEEE*

Abstract—WSe₂ p-MOSFETs with Nb-doped WS₂ contacts formed using atomic layer deposition are demonstrated. The devices are fabricated using a technique that aligns the contact metallization with the Nb-doped WS₂ contacts using a selective oxidation process. Devices with source/drain spacing of 0.15 μ m have on-state current of 103 μ A/ μ m at V_{DS} = -1 V at a channel carrier concentration of ~ 7.5 × 10¹² cm⁻². The results provide a promising CMOS-compatible pathway to create low-resistance contacts to 2D-channel transistors.

Index Terms – WSe₂, transition metal dichalcogenide, 2D semiconductor, MOSFET.

I. INTRODUCTION

Two-dimensional (2D) transition metal dichalcogenides (TMDs) are promising semiconductors for future scaled CMOS technologies due to their atomically thin channels, which allow excellent electrostatic control and improved scalability compared to silicon [1]. Among these, tungsten diselenide (WSe₂) is particularly suited for p-channel devices since it offers a suitable bandgap (~1.2 eV in monolayer form), high hole mobility, and a relatively shallow valence band edge, making p-type contacts more achievable [2].

Despite significant progress on WSe₂ p-MOSFETs, device performance remains limited by high contact resistance. Reliable hole injection is difficult due to strong Fermi-level pinning from metal-induced gap states and the lack of suitable semi-metallic contact materials. Techniques such as surface doping [3], insertion of interfacial layers [4], and use of high—work function metals [5] or oxides [6] have improved performance but often suffer from poor scalability, limited thermal stability, or incompatibility with CMOS processing [7].

A promising route to low-resistance contacts is Nb-doped layers [8]. Substitutional Nb doping during channel growth can produce degenerate p-type behavior with hole densities up to 10^{19} – 10^{20} cm⁻³ [9]. However, direct channel doping does not allow independent control of the contact resistance, $R_{\rm C}$, and threshold voltage. Another strategy is 2D/2D contact stacks using metallic TMDs such as NbSe₂, TaS₂, or alloyed WSe₂ [10],[11]. These methods highlight the benefits of heavy p-type doping at the contact interface but typically rely on exfoliated flakes, transfers, or co-growth [12], which are not scalable to wafer-level integration.

Atomic layer deposition (ALD) offers a scalable alternative, providing conformal coverage, wafer-scale uniformity, and angstrom-level thickness control [13]. ALD can incorporate

This work was partially funded by Intel Corporation, and also by the University of Minnesota College of Science and Engineering. Portions of this work were conducted in the Minnesota Nano Center, which is supported by the NSF through the National Nanotechnology Coordinated Infrastructure under Award No. ECCS-2025124, and the University of Michigan Lurie Nanofabrication Facility. S. Mishra is with the Dept. of Electrical & Computer

metal precursors to form degenerately-doped TMD alloys. Nb has proven effective as a substitutional dopant in WSe2 and MoS2 [14], and Nb-enriched WS2 grown by ALD has shown high conductivity with hole densities exceeding $10^{20}\,\rm cm^{-3}$ [15],[16]. Such films act as high-work-function, p*-type layers that can transfer charge into adjacent semiconductors, enabling efficient hole injection. Despite these advantages, ALD-based doped interlayers have not yet demonstrated in WSe2 PFETs.

In this work, we demonstrate a scalable, self-aligned contact doping strategy using plasma-enhanced ALD (PEALD) of Nb-doped WS₂ (Nb:WS₂) as a raised source/drain contact layer. Devices with contact spacing, $L_{\rm DS}$, of 0.15 μ m exhibit a drive current of > 100 μ A/ μ m at $V_{\rm DS}=-1$ V and $n_{\rm s}=7.5\times10^{12}$ cm⁻². A self-aligned contact process using O₂ annealing ensures precise alignment of Nb:WS₂ to Pd contacts while maintaining excellent channel transport. The use of PEALD as a contact strategy is a promising path toward a manufacturing-compatible 2D transistor process.

II. DEVICE FABRICATION

The device fabrication started with degenerately doped p⁺⁺ Si wafers with 90-nm thermally grown SiO₂, used as global backgate substrates. Prior to transferring exfoliated WSe₂, the substrates were cleaned by sequential rinsing in acetone, isopropanol, and deionized water, dried with N₂, and exposed to brief O₂ plasma to remove organics. WSe₂ flakes of monolayer (1L), bilayer (2L), and few-layer (FL) thicknesses were exfoliated from bulk crystals and transferred onto the substrates. Optical microscopy identified suitable flakes, and thicknesses were verified by Raman spectroscopy. A conformal Nb:WS₂ (Nb/W ratio \approx 0.43) was then deposited by PEALD at 300 °C [15]. Each super-cycle consisted of four W cycles and one Nb cycle, yielding a ~1.6-nm-thick film coating the WSe₂ and surrounding oxide.

Device fabrication proceeded by defining transistor mesas with SF_6/O_2 reactive ion etching and patterning Pd (20 nm)/Au (50 nm) contacts by electron-beam lithography, evaporation and lift-off. The backside oxide was etched in buffered oxide etchant for 2 min to expose the p^{++} Si for to allow backgate contact. FIG. 1 shows a schematic of the fabrication sequence.

Samples were characterized before and after O₂ annealing at 200 °C for 20 min. During the annealing step, the Nb:WS₂ in the channel regions oxidizes forming an amorphous insulating layer [17], as confirmed by electrical tests in regions without WSe₂, while the film beneath the contacts remained intact,

Engineering, University of Minnesota, Minneapolis, MN, USA A. A. Adhikari, and S. J. Koester are with the Dept. of Electrical Engineering, University of Notre Dame, Notre Dame, IN, USA (e-mail: skoester@nd.edu). A. A. Bol, L. G. Cooper, and R. A. Dawley are with the Dept. of Chemistry, University of Michigan, Ann Arbor, MI, USA. D. Seo is now with Argonne National Laboratory, R. Li is now with Micron Technology.

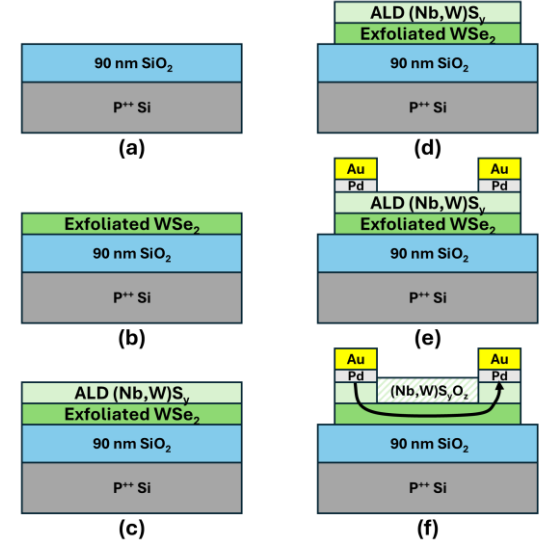


FIG. 1. Process flow for WSe₂ p-MOSFETs. (a) Starting substrate, (b) exfoliation of WSe₂, (c) PEALD deposition of Nb:WS₂, (d) mesa patterning, (e) lift-off of Pd/Au ohmic contact metallization, (f) selective oxidation of Nb:WS₂. The arrow shows the current transport path after the oxidation step.

creating self-aligned doped source/drain regions. Electrical characterization before and after RTA/O₂ was performed at room temperature in a vacuum probe station (<10⁻⁵ Torr) using a Keysight B1500A semiconductor parameter analyzer, with the p⁺⁺ Si substrate as the back gate. Transfer and output characteristics were recorded before and after annealing for direct comparison across 1L, 2L, and FL WSe₂ devices.

III. RESULTS AND DISCUSSION

FIG. 2 shows the results for devices with $L_{\rm DS} = 0.6 \, \mu \rm m$ with 1L, 2L and FL WSe₂ channels both before and after O₂ annealing. We also include the results for a device where the Nb:WS₂ was deposited directly on the SiO₂ substrate, and we label this device as 0L. Before anneal (FIG. 2(a)) it is clear that no devices have strong turn-off behavior. This is expected given that the Nb:WS₂ shorts the source and drain together and is only poorly modulated by the bottom-gate electrode. However, we do note that the results are affected by the number of WSe₂ layers, with the on-state current increasing as the number of WSe₂ layers is increased. As we described in previous work, this is strong evidence that charge transfer is taking place between the Nb:WS₂ layer and the WSe₂ channel [16]. Since transport is dominated by the bottom-most WSe₂ layer due to the backgating effect, greater number of layers increases the distance between the channel and the polycrystalline Nb:WS₂ layer. We also note that the FL device has much larger hysteresis than the other devices. While the origin of this is not completely clear, we believe this is due to charge trapping in the WSe₂ itself.

After annealing, the devices show very different behavior as shown in FIG. 2(b). First of all, we found that the 0L samples become completely insulating with current level below the noise floor of our measurements, and so these results are not shown. For 1L-WSe₂, the on-off current ratio increases substantially from \sim 3 to nearly 6×10^3 . This is attributed to the oxidation of the Nb:WS₂ between the S/D, which renders it

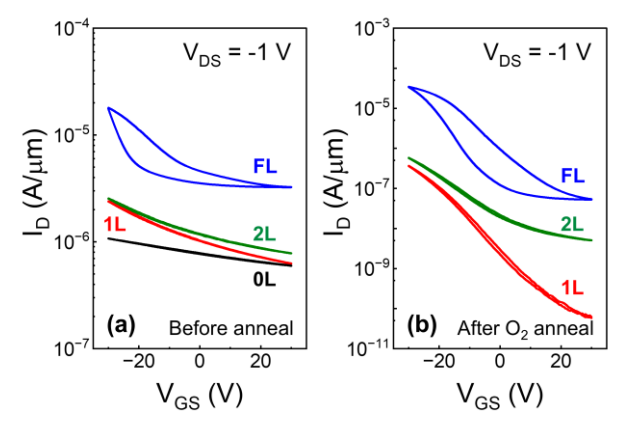


FIG. 2. (a) Plot of drain current, I_D , vs. gate-to-source voltage, $V_{\rm GS}$, for 0L, 1L, 2L and FL WSe₂ p-MOSFETs before oxidation of the Nb:WS₂ layer. (b) $I_{\rm D}$ vs. $V_{\rm GS}$ for same devices in (a) after RTA/O₂ at 200 °C for 20 min. The curves for the 0L devices had current below the noise floor and are not shown. For all devices, $L_{\rm DS} = 0.6~\mu{\rm m}$, and data was taken at room temperature.

insulating, thus removing the shunt leakage path between the S/D contacts. However, the on-state current is also reduced dramatically, decreasing by roughly a factor of 10. A similar situation is observed for the 2L-WSe₂ sample, though the on-off current ratio is lower than for 1L-WSe₂. Since the Nb:WS₂ is deposited using PEALD, we attribute the reduced performance to mobility degradation of the channel due to plasma-induced damage.

After oxidation, the result for the FL-WSe₂ sample is very different. Here, the on-state current actually increases after O_2 annealing, going from 18 $\mu A/\mu m$ to 34 $\mu A/\mu m$. Due to much larger thickness of the WSe₂ channel, we believe the bottom WSe₂ is protected from the plasma damage, allowing the transport properties to be closer to the values for pristine material. The on-off current ratio for the FL-WSe₂ device is also improved, going from ~ 5.5 to over 600.

Given the improved performance of the FL-WSe₂ devices, we performed additional experiments to study the contact-spacing dependence and the results are shown in FIG. 3. Here, devices with $L_{\rm DS} = 0.6$, 0.4, 0.2 and 0.15 µm were tested. Before O₂ annealing, the devices showed similar behavior to those in FIG. 2. After annealing, the devices show increasing drive current, with values of 34, 43, 96, and 103 µA/µm, at $V_{\rm GS} = -30$ V and $V_{\rm DS} = -1$ V (FIG. 3(a)). The devices all show similar

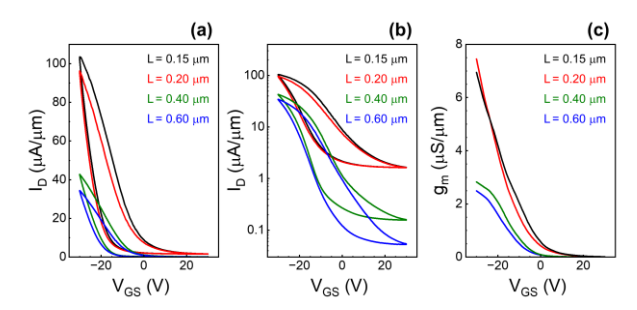


FIG. 3. (a) Plot of drain current, I_D , vs. gate-to-source voltage, $V_{\rm GS}$, on a linear scale for FL WSe₂ p-MOSFETs with different source/drain contact spacing, $L_{\rm DS}$, at $V_{\rm DS} = -1$ V. (b) Same plot as in (a) except on a semi-log plot. (c) Transconductance, $g_{\rm m}$, vs. $V_{\rm GS}$, where $g_{\rm m}$ is averaged between up and down sweeps.

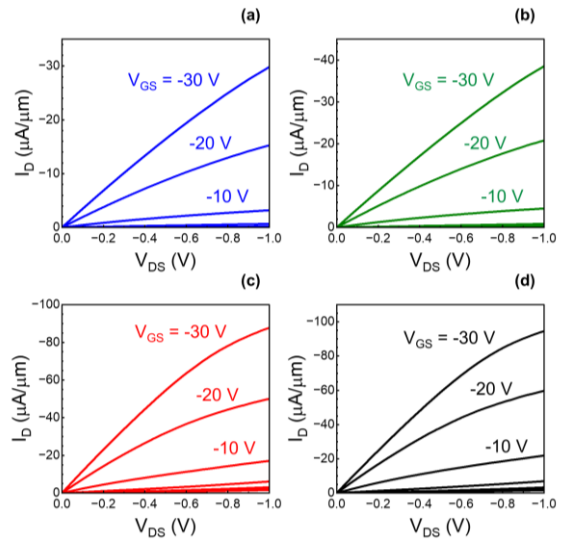


FIG. 4. Output characteristics for FL WSe₂ p-MOSFETs with source/drain contact spacing, $L_{\rm DS}$, of (a) 0.6 μ m, (b) 0.4 μ m, (c) 0.2 μ m, and (d) 0.15 μ m.

hysteresis and turn-off behavior, though the on-off current ratio decreases slightly with shorter channel length (FIG. 3(b)). The transconductance, $g_{\rm m}$, also increases going from $L_{\rm DS}=0.6$ to 0.2 μ m, but then decreases slightly at $L_{\rm DS}=0.15~\mu$ m (FIG. 3(c)). This could be a result of short-channel effects, but may also indicate the onset of contact-limited performance.

The output characteristics of the same devices are shown in FIG. 4. All devices show linear turn-on, indicative of ohmic contacts. The on-state currents are slightly different than those in FIG. 3, which we attribute to the hysteretic nature of the backgate, which often can cause variations in current depending upon how the device is swept. For the $L_{\rm DS}=0.15$ -µm device, the average threshold voltage between up and down sweeps is +1 V, and so at $V_{\rm GS}=-30$ V, $n_{\rm s}=7.5\times10^{12}$ cm⁻². Furthermore, based upon the maximum $g_{\rm m}$ value in FIG. 3(c), we extract a field-effect mobility of 21 cm²/Vs for the $L_{\rm DS}=0.6$ µm device.

Our results compare favorably with previous reports in the literature on WSe₂ p-MOSFETs [18]-[37], as summarized in FIG. 5. Here, we have plotted our figure of merit (FOM), $I_{\rm ON}$ / $n_{\rm s}$ vs. gate length, where our FOM accounts for devices under different gating conditions. Our results compare favorably with

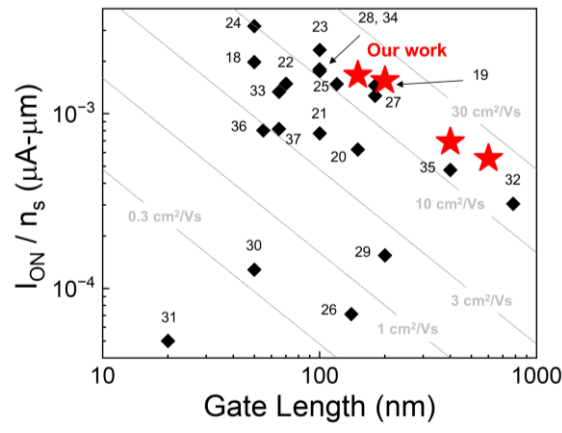


FIG. 5. Plot at $V_{\rm DS} = -1$ V showing our work (red stars) compared to WSe₂ p-MOSFETs in the literature [18]-[37]. Gray dashed lines show expected trends for $I_{\rm ON}/n_{\rm s}$ at different mobility values.

most reports in the literature, providing strong evidence of the benefit of ALD-based doping for contact formation, particularly given the CMOS-compatibility of our ALD scheme relative to other techniques.

IV. CONCLUSION

In conclusion, we have demonstrated a technique to form contacts to 2D p-MOSFETs using Nb:WS₂ contacts formed using PEALD. The devices are fabricated using a technique that aligns the contact metallization with the Nb:WS₂ using a selective oxidation process. Devices with source/drain spacing of 0.15 μ m have on-state current of 103 μ A/ μ m at $V_{DS} = -1$ V and $n_s \sim 7.5 \times 10^{12}$ cm⁻². The work demonstrates the potential of ALD TMDs as a contact solution for ultra-scaled CMOS.

REFERENCES

- K. P. O'Brien, C. H. Naylor, C. Dorow, et al., "Process Integration and Future Outlook of 2D transistors," *Nat. Commun.*, vol. 14, Art. No. 6400, Oct. 2023. doi: doi.org/10.1038/s41467-023-41779-5
- [2] H. Fang, S. Chuang, T. C. Chang, K. Takei, T. Takahashi, and A. Javey, "High-Performance Single-Layered WSe₂ p-FETs with Chemically Doped Contacts," *Nano Lett.*, vol. 12, no. 7, pp. 3788–3792, Jun. 2012. doi: 10.1021/nl301702r
- [3] I. Kim, N. Higashitarumizu, I. K. M. R. Rahman, S. Wang, H. M. Kim, J. Geng, R. R. Prabhakar, J. W. Ager III, and A. Javey, "Low Contact Resistance WSe₂ p-Type Transistors with Highly Stable, CMOS-Compatible Dopants," *Nano Lett.*, vol. 24, pp. 13528–13533, Oct. 2024. doi: 10.1021/acs.nanolett.4c02948
- [4] S. Chuang, C. Battaglia, A. Azcatl, S. McDonnell, J. S. Kang, X. Yin, M. Tosun, R. Kapadia, H. Fang, R. M. Wallace, and A. Javey, "MoS₂ P-Type Transistors and Diodes Enabled by High Work Function MoO_x Contacts," *Nano Lett.*, vol. 14, pp. 1337–1342, 2014. doi: 10.1021/nl4043505
- [5] N. H. Patoary, J. Xie, G. Zhou, M. A. Rahman, T. Chen, and S. Y. Chung, "Improvements in 2D p-Type WSe₂ Transistors Towards Ultimate CMOS Scaling," Sci. Rep., vol. 13, Art. no. 3304, Feb. 2023. doi: 10.1038/s41598-023-30317-4
- [6] S. Yang, G. Lee, and J. Kim, "Selective p-Doping of 2D WSe₂ via UV/Ozone Treatments and its Application in Field-Effect Transistors," ACS Appl. Mater. & Interfac., vol. 13, pp. 955–961, Jan. 2021. doi: 10.1021/acsami.0c19712
- [7] M. Lanza, Q. Smets, C. Huyghebaert, and L. J. Li, "Yield, Variability, Reliability, and Stability of Two-Dimensional Materials Based Solid State Electronic Devices," *Nat. Commun.*, vol. 11, Art. no. 5689, 2020. doi: 10.1038/s41467-020-19053-9
- [8] S. K. Pandey, H. Alsalman, J. G. Azadani, N. Izquierdo, T. Low, and S. A. Campbell, "Controlled p-Type Substitutional Doping in Large-Area Monolayer WSe₂ Crystals Grown by Chemical Vapor Deposition, Nanoscale, vol. 10, pp. 21374–21385, Nov. 2018. doi: 10.1039/C8NR07070A
- [9] J. Suh, T.-E. Park, D.-Y. Lin, et al., "Doping Against the Native Propensity of MoS₂: Degenerate Hole Doping by Substitutional Nb," Nano Lett., vol. 14, pp. 6976–6982, Dec. 2014. doi: 10.1021/nl503104p
- [10] D. Cui, S. Shen, W. Wu, W. Chen, X. Zhou, J. Han, X. Yue, J. Li, R. Liu, L. Hu, C. Cong, and Z.-J. Qiu, "Two-Dimensional 2H-TaS2 Contact for Fermi-Level-Pinning-Free p-Type WSe2 Field-Effect Transistors," ACS Appl. Mater. & Interfac., vol. 17, pp. 55213–55221, Sep. 2025, doi: 10.1021/acsami.5c125029
- [11] H. J. Chuang, B. Chamlagain, M. Koehler, M. M. Perera, J. Yan, D. Mandrus, D. Tomanek, and Z. Zhou, "Low Resistance 2D/2D Ohmic Contacts: A Universal Approach to High Performance WSe₂, MoS₂, and MoSe₂ Transistors," *Nano Lett.*, vol. 16, pp. 1896–1902, 2016. doi: 10.1021/acs.nanolett.5b05066
- [12] T. Schram, S. Sutar, I. Radu, and I. Asselberghs, "Challenges of Wafer-Scale Integration of 2D Semiconductors for High-Performance Transistor Circuits," Adv. Mater., vol. 34, Art. no. 2109796, 2022. doi: 10.1002/adma.202109796
- [13] X. Guo, H. Yang, X. Mo, R. Bai, Y. Wang, Q. Han, S. Han, Q. Sun, D. W. Zhang, S. Hu, and L. Ji, "Modulated Wafer-Scale WS₂ Films Based on Atomic-Layer-Deposition for Various Device Applications," RSC Adv., vol. 13, pp. 14841–14848, May 2023. doi: 10.1039/D3RA00933E

- [14] V. Vandalon, M. A. Verheijen, W. M. M. Kessels, and A. A. Bol, "Atomic Layer Deposition of Al-Doped MoS₂: Synthesizing a p-Type 2D Semiconductor with Tunable Carrier Density," ACS Appl. Nano Mater., vol. 3, pp. 10200–10208, 2020. doi: 10.1021/acsanm.0c02167
- [15] J. J. P. M. Schulpen, C. H. X. Lam, R. A. Dawley, R. Li, L. Jin, T. Ma, W. M. M. Kessels, S. J. Koester, and A. A. Bol, "Nb Doping and Alloying of 2D WS₂ by Atomic Layer Deposition for 2D Transition-Metal Dichalcogenide Transistors and HER Electrocatalysts," ACS Appl. Nano Mater., vol. 7, pp. 7395–7407, Apr. 2024. doi: 10.1021/acsanm.4c00094
- [16] R. Li, J. J. P. M. Schulpen, R. A. Dawley, N. Hirshberg, M. L. Odlyzko, S. Lee, K. S. Hoque, T. Low, A. S. McLeod, A. A. Bol, and S. J. Koester, "Ultralow-Resistance Contacts to Heavily Doped p-Type Nb_xW_{1-x}S_y Thin Films Grown by Atomic Layer Deposition," ACS Appl. Mater. & Interfac., vol. 17, pp. 10931–10941, Feb. 2025. doi: 10.1021/acsami.4c16889
- [17] R. Li, R. A. Dawley, S. Mishra, A. Adhikari, A. A. Bol, and S. J. Koester, "WS₂ p-MOSFETs with Channels Deposited by Plasma-Enhanced Atomic-Layer Deposition," *Appl. Phys. Lett.*, vol. 126, Art. no. 253102, Jun. 2025. doi: 10.1063/5.0267728
- [18] S. Chen, Y. Zhang, W. P. King, R. Bashir, and A. M. van der Zande, "Extension Doping with Low-Resistance Contacts for p-Type Monolayer WSe₂ Field-Effect Transistors," *Adv. Electron. Mater.*, vol. 11, Art. no. 2400843, Jun. 2025. doi: 10.1002/aelm.202400843
- [19] H. Y. Lan, Y. Tan, S. H. Yang, X. Liu, Z. Shang, J. Appenzeller, and Z. Chen, "Improved Hysteresis of High-Performance p-Type WSe₂ Transistors with Native Oxide WO_x Interfacial Layer," *Nano Lett.*, vol. 25, pp. 5616–5623, 2025. doi: 10.1021/acs.nanolett.4c06060
- [20] Y. Tan, S. H. Yang, C. P. Lin, F. J. Vega, J. Cai, H. Y. Lan, R. Tripathi, S. Sharma, Z. Shang, T. H. Hou, T. E. Beechem, J. Appenzeller, and Z. Chen, "Monolayer WSe₂ Field-Effect Transistor Performance Enhancement by Atomic Defect Engineering and Passivation," ACS Nano, vol. 19, pp. 8916–8925, 2025. doi: 10.1021/acsnano.4c16831
- [21] K. Maxey, C. H. Naylor, K. P. O'Brien, A. Penumatcha, A. Oni, C. Mokhtarzadeh, C. J. Dorow, C. Rogan, B. Holybee, T. Tronic, D. Adams, N. Arefin, A. S. Gupta, C. C. Lin, T. Zhong, S. Lee, A. Kitamura, R. Bristol, S. B. Clendenning, U. Avci, and M. Metz, "300 mm MOCVD 2D CMOS Materials for More (Than) Moore Scaling," in *Proc. IEEE Symp. VLSI Technol. Circ.*, Honolulu, HI, USA, 2022, pp. 419–420. doi: 10.1109/VLSITechnologyandCir46769.2022.9830457
- [22] A. Penumatcha, K. P. O'Brien, K. Maxey, et al. "High Mobility TMD NMOS and PMOS Transistors and GAA Architecture for Ultimate CMOS Scaling," in *Proc. IEEE Int. Elect. Dev. Meeting (IEDM)*, San Francisco, CA, USA, 2023, pp. 1–4. doi: 10.1109/IEDM45741.2023.10413662
- [23] X. Wang, X. Shi, X. Xiong, R. Huang, and Y. Wu, "BEOL Compatible High-Performance Monolayer WSe2 pFETs With Record $G_m=190~\mu S/\mu m$ and $I_{on}=350~\mu A/\mu m$ by Direct-Growth on SiO2 Substrate at Reduced Temperatures," in *Proc. IEEE Int. Elect. Dev. Meeting (IEDM)*, San Francisco, CA, USA, 2023, pp. 1–4. doi: 10.1109/IEDM45741.2023.10413833
- [24] A. S. Chou, C. H. Hsu, Y. T. Lin, et al., "Status and Performance of Integration Modules Toward Scaled CMOS With Transition Metal Dichalcogenide Channel," in *Proc. IEEE Int. Elect. Dev. Meeting* (*IEDM*), San Francisco, CA, USA, 2023, pp. 1–4. doi: 10.1109/IEDM45741.2023.10413779
- [25] X. Shi, X. Wang, S. Liu, Q. Guo, L. Sun, X. Li, R. Huang, and Y. Wu, "High-Performance Bilayer WSe₂ pFET With Record $I_{ds}=425~\mu A/\mu m$ and $G_m=100~\mu S/\mu m$ at $V_{ds}=-1~V$ by Direct Growth and Fabrication on SiO₂ Substrate," in *Proc. IEEE Int. Elect. Dev. Meeting (IEDM)*, San Francisco, CA, USA, 2022, pp. 7.1.1–7.1.4. doi: 10.1109/IEDM45625.2022.10019404
- [26] C. J. Dorow, T. Schram, Q. Smets, et al., "Exploring Manufacturability of Novel 2D Channel Materials: 300 mm Wafer-Scale 2D NMOS and PMOS Using MoS₂, WS₂, and WSe₂," in *Proc. IEEE Int. Elect. Dev. Meeting (IEDM)*, San Francisco, CA, USA, 2023, pp. 1–4. doi: 10.1109/IEDM45741.2023.10413874
- [27] H. Y. Lan, R. Tripathi, X. Liu, J. Appenzeller, and Z. Chen, "Wafer-Scale CVD Monolayer WSe₂ p-FETs With Record-High 727 μA/μm I_{on} and 490 μS/μm G_{max} via Hybrid Charge Transfer and Molecular Doping," in *Proc. IEEE Int. Elect. Dev. Meeting (IEDM)*, San Francisco, CA, USA, 2023, pp. 1–4. doi: 10.1109/IEDM45741.2023.10413736
- [28] A. S. Chou, Y. T. Lin, Y. C. Lin, et al., "High-Performance Monolayer WSe₂ p/n FETs via Antimony–Platinum Modulated Contact Technology Toward 2D CMOS Electronics," in *Proc. IEEE Int. Elect. Dev. Meeting* (*IEDM*), San Francisco, CA, USA, 2022, pp. 7.2.1–7.2.4. doi: 10.1109/IEDM45625.2022.10019491

- [29] K. P. O'Brien, C. J. Dorow, A. Penumatcha, et al., "Advancing 2D Monolayer CMOS Through Contact, Channel and Interface Engineering," in *Proc. IEEE Int. Elect. Dev. Meeting (IEDM)*, San Francisco, CA, USA, 2021, pp. 7.1.1–7.1.4. doi: 10.1109/IEDM19574.2021.9720651
- [30] W. Mortelmans, P. Buragohain, C. Rogan, et al., "Record Performance in GAA 2D NMOS and PMOS Using Monolayer MoS₂ and WSe₂ with Scaled Contact and Gate Length," in *Proc. IEEE Symp. VLSI Technol. Circ.*, Honolulu, HI, USA, 2024, pp. 1–2. doi: 10.1109/VLSITechnologyandCir46783.2024.10631395
- [31] A. Oberoi, Y. Han, S. P. Stepanoff, et al., "Toward High-Performance p-Type Two-Dimensional Field-Effect Transistors: Contact Engineering, Scaling, and Doping," ACS Nano, vol. 17, pp. 19709–19723, 2023. doi: 10.1021/acsnano.3c03060
- [32] C. Dorow, K. O'Brien, C.H. Naylor, S. Lee, A. Penumatcha, A. Hsiao, T. Tronic, M. Christenson, K. Maxey, H. Zhu, A. Oni, U. Alaan, T. Gosavi, A.S. Gupta, R. Bristol, S. Clendenning, M. Metz, and U. Avci, "Advancing Monolayer 2D nMOS and pMOS Tansistor Integration From Growth to van der Waals Interface Engineering for Ultimate CMOS Scaling," *IEEE Trans. Elect. Dev.*, vol. 68, pp. 6592–6598, 2021. doi: 10.1109/TED.2021.3118659
- [33] C. S. Pang, T. Y. T. Hung, A. Khosravi, R. Addou, Q. Wang, M. Kim, R. M. Wallace, and Z. Chen, Z, "Atomically Controlled Tunable Doping in High-Performance WSe₂ Devices," *Adv Electron. Mater.*, vol. 6, 1901304, Aug. 2020. doi: 10.1002/aelm.201901304
- [34] S. Ghosh, M. U. K. Sadaf, A. R. Graves, Y. Zheng, A. Pannone, S. Ray, C. Y. Cheng, J. Guevara, J. M. Redwing, and S. Das, "High-Performance p-Type Bilayer WSe₂ Field Effect Transistors by Nitric Oxide Doping," *Nat. Commun.*, vol. 16, Art. No. 5649, Jul. 2025. doi: 10.1038/s41467-025-59684-4
- [35] N. H. Patoary, J. Xie, G. Zhou, F. Al Mamun, M. Sayyad, S. Tongay, and I. S. Esqueda, "Improvements in 2D P-Type WSe₂ Transistors Towards Ultimate CMOS Scaling," *Sci Rep.*, vol. 13, Art. No. 3304, Feb. 2023. doi: 10.1038/s41598-023-30317-4
- [36] H. Y. Lan, C. P. Lin, L. Liu, J. Cai, Z. Sun, P. Wu, Y. Tan, S. H. Yang, T. H. Hou, J. Appenzeller, and Z. Chen, "Uncovering the Doping Mechanism of Nitric Oxide in High-Performance P-Type WSe₂ Transistors," *Nat. Commun.*, vol. 16, Art. No. 4160, May 2025. doi: 10.1038/s41467-025-59423-9
- [37] C. C. Chiang, H. Y. Lan, C. S. Pang, J. Appenzeller, and Z. Chen, "Air-Stable P-Doping in Record High-Performance Monolayer WSe₂ Devices," *IEEE Elect. Dev. Lett.*, vol. 43, pp. 319–322, Feb. 2022. doi: 10.1109/LED.2021.3135312.